Published May 7, 2019

Original Research

Core Ideas

- Transversal relaxation time spectra were a good proxy to determine pore size distribution.
- Chitosan provides more degradable C to the soil microbial community than Arabic gum.
- The water retention curve showed that 10 g Arabic gum kg^{-1} soil decreased plant-available water.
- The same amount of chitosan increased available water content compared with the reference soil.

Water Retention and Pore Size Distribution of a Biopolymeric-Amended Loam Soil

Mehdi Rahmati,* Andreas Pohlmeier, Sara Mola Ali Abasiyan, Lutz Weihermüller, and Harry Vereecken

The pore size distribution (PSD) of biopolymeric-amended soils is rarely investigated due to difficulties in its quantification using classical methods. In this study, we analyzed the impact of biopolymeric soil amendments on the PSD of a dryland loamy soil based on its physical and biological properties using a completely randomized design with four treatments consisting of two different dosages (10 and 5 g kg^{-1}) of two different biopolymers, (chitosan [CH] and Arabic gum [AG]) plus a reference soil. To determine the effects of CH and AG on the PSD, nuclear magnetic resonance relaxometry (NMRR) measurements were used to determine the longitudinal (T_1) and transversal (T_2) relaxation times. A set of soil structure–related characteristics was also determined in the laboratory. The results revealed that T_2 spectra provided a good proxy to determine the PSD, showing good agreement between the PSD from T_2 spectra and that calculated from the water retention curve (WRC) (R^2 > 0.78; RMSE <1.38 μm). The application of CH also increased the zeta potential of the soil to −18.5 mV, compared with −20 mV obtained for the reference soil. The WRC measurements revealed that AG decreased the available water content for plant use compared with the reference soil, whereas CH increased the available water in comparison to the reference soil. Considering the parameters of the van Genuchten model, the application of AG and CH mainly affected the parameter α, confirming the dominant changes in macropores. This finding was confirmed by NMRR relaxation spectra. Furthermore, the application of CH and AG stimulated the microbial activity of the amended soil, leading to an increase in soil respiration.

Abbreviations: AG, Arabic gum; CPMG, Carr–Purcell–Meiboom–Gill; CH, chitosan; EC, electrical conductivity; HL, half-life; MRT, mean residence time; MWD, mean weight diameter of aggregates; NMRR, nuclear magnetic resonance relaxometry; OC, organic carbon; PSD, pore size distribution; SA, soil amendment; T_1, longitudinal relaxation time; T_2, transversal relaxation time; WRC, water retention curve; WAS, wet-aggregate stability.

M. Rahmati and S.M.A. Abasiyan, Dep. of Soil Science and Engineering, Faculty of Agriculture, Univ. of Maragheh, Maragheh, Iran; M. Rahmati, A. Pohlmeier, L. Weihermüller, and H. Vereecken, Forschungszentrum Jülich GmbH, Institute of Bio- and Geosciences: Agrosphere (IBG-3), 52428 Jülich, Germany. *Corresponding author (mehdirmti@gmail.com).

Received 26 Nov. 2018.
Accepted 22 Jan. 2019.

Citation: Rahmati, M., A. Pphlmeier, S.M.A. Abasiyan, L. Weihermüller, and H. Vereecken. 2019. Water retention and pore size distribution of a biopolymeric-amended loam soil. Vadose Zone J. 18:180205. doi:10.2136/vzj201811.0205

The soil amendments (SAs), which are materials applied to the soil surface or incorporated into the surface layer to improve soil water retention characteristics, comprise a class of materials that can be organic (manure, compost, biopolymers, biochar, etc.), inorganic (lime, gypsum, etc.), synthesized (super-absorbents, polymers, and some kinds of biopolymers), and industrial byproducts (slag, mud, digestate, etc.) (Blanco-Canqui and Lal, 2008). Although the use of SAs has gained considerable interest in recent years (Blanco-Canqui and Lal, 2008), to o our knowledge, few attempts have been made to investigate the changes in the pore size distribution (PSD) of amended soils.

The fraction of soil volume that is not occupied by solid material is considered as soil pore space, and the relative abundance of each pore size in a representative volume of soil is considered as PSD (Shi et al., 2017). Pore size distribution is a fundamental and key parameter in transmission and storage of soil water and solute (Mallants et al., 1997; Lipiec and Stepniewski, 1995), soil aeration, and root growth (Pagliai and Vignozzi, 2002; Valentine et al., 2012). Kutilek (2004) categorized pores into three groups according to the laws of hydrostatics and hydrodynamics (Kutilek and Nielsen, 1994): (i) submicroscopic pores, (ii) micropores or capillary pores, and (iii) macropores or noncapillary pores. In general, submicroscopic pores are considered too small to conduct water or to form continuous water flow paths (Kutilek, 2004). Micropores may occur in either within (intra-aggregate)

and between aggregates (interaggregate) or within blocks of soil particles if aggregates are not present (Kutilek, 2004). Macropores may occur in interaggregate spaces (Jullien et al., 2005) and/or in decayed roots, earthworm channels, fissures, and cracks (Kutilek, 2004). Macropores are defined as pores that do not form capillary menisci and therefore do not retain water against gravitation. Kutilek (2004) considered an equivalent pore radius of 15 to 30 μm (mean, 23 μm) as an approximate threshold between intraaggregate and interaggregate pores and 1000 to 1500 μm (mean, 1250 μm) as an approximate threshold between micropores and macropores. For clay-rich materials, Jullien et al. (2005) also classified pores into interlayer, interparticle, and interaggregate (macro) pores. To merge these two classifications, we assume that submicroscopic pores introduced by Kutilek (2004) correspond to the interlayer pores defined by Jullien et al. (2005). In this class of pores (on nanoscale), the water molecules are retained in the interlayer spaces of clays or associated with clay particles. Therefore, we use the term *interlayer pores* for these types of pores. We use the term *capillary pores* for intra-aggregate and intraparticle pores (with $d < 23$ μm, where d is pore radius) and interaggregate pores (with 23 μm $< d <$ 1250 μm) where capillary menisci are formed. The term *macropores* refers to larger interaggregate pores (with $d >$ 1250 μm) where capillary menisci are not formed.

The study of the impact on PSD is usually neglected in soil amendment experiments because it is difficult to quantify by classical field/laboratory methods, including direct or indirect measurement of PSD from water retention curve (WRC) measurements based on soil water content or geophysical measurements and hydrological inversion (as done by Jadoon et al., 2012; Busch et al., 2013; and Jonard et al., 2015) or WRC measured by pressure plate extractors (e.g., Bittelli and Flury, 2009); multistep outflow (e.g., Bayer et al., 2005; Hollenbeck and Jensen, 1998; Neyshabouri et al., 2013; Weihermüller et al., 2009); or the evaporation (e.g., Schindler et al., 2010; Žydelis et al., 2018), mercury intrusion (e.g., Webb, 2001), and nitrogen sorption (e.g., Kowalczyk et al., 2003) methods. As an alternative, noninvasive measurement techniques can be used, such as MicroCT (e.g., Koestel, 2018; Pohlmeier et al., 2018; Smet et al., 2017), synchrotron radiation and/or microtomography (e.g., Peth et al., 2008), or nuclear magnetic resonance relaxometry (NMRR) (e.g., Jaeger et al., 2009; Stingaciu et al., 2010).

Nuclear magnetic resonance relaxometry has been successfully applied in studying the characteristics of the pore space in geological porous media like sandstone rocks (Kleinberg et al., 1994; Song, 2010) as well as natural soils (Brax et al., 2017; Hall et al., 1997; Hinedi et al., 1993; Pohlmeier et al., 2009). According to the empirical model of Brownstein and Tarr (1977, 1979), the observable relaxation rates are composed of the bulk rate plus a term describing enhanced surface relaxation. Because the average collision rate of water with the pore wall is higher in small pores than in large pores due to shorter translational diffusive pathways, the overall rate is faster, and one observes a linear relation between relaxation rate and reciprocal pore size. This relation allows the calculation of PSD from relaxation time distribution (Barrie, 2000; Hinedi et al., 1997; Ryu, 2009). In this regard, Morriss et al. (1997) compared the NMRR spectra with independently obtained PSD by mercury injection porosity measurements, leading to a classification of NMR-derived pore sizes for sandstones, where the transversal relaxation times (T_2) of 3 and 33 ms were considered as cutoff values to separate clay-bound water, capillary-bound water, and free water fractions. Later, Bird et al. (2005) compared WRCs with longitudinal relaxation time distribution (T_1) functions of model porous media and three natural soils. From bimodal distribution functions, they determined intra-aggregate and bulk water, which are characterized by short and long T_1 values ranging from 3 to 100 ms. The direct scaling of NMR relaxation time to pore size was discussed by Jaeger et al. (2009), who found better correlation between PSD and T_2 spectra by using a dual-relaxivity model, which defines separate surface relaxivity parameters for micropores and mesopores. Recently, Meyer et al. (2018) confirmed this approach by calibration and validation with 14 different soil materials. They found T_2 surface relaxivities of 551.7 and 9.6 μm s^{-1} for macro- and medium-sized pores defined by matrix potentials of approximately −32 kPa. The T_2 spectra also correlate with wet-aggregate stability (WAS) and average particle size. Buchmann et al. (2015) differentiated between clay-associated water, micropores, and mesopores and macropores by defining T_2 cutoff values of 3, 60, and 300 ms, respectively, and discussed the correlation of WAS, particle size, and T_2 spectra. Recently, Shi et al. (2017) discussed the concept of separating pore size classes in swelling soil materials into clay interlayer, interparticle, and interaggregate pores, separated by T_2 values of 10 and 100 ms.

In addition to the lack of the studies on the effects of different SAs on the PSD, there is a lack of studies on the use of natural biopolymers as SAs because most of the investigated biopolymers have a synthetic origin rather than being natural (Awad et al., 2013; Chang and Cho, 2012; Chang et al., 2015a, 2015b; Maghchiche et al., 2010; Orts et al., 2007). Natural biopolymers, such as Arabic gum (AG), agar, cellulose, alginate, psyllium gaur gum, bacterial exopolysaccharide, and chitosan (CH), have been investigated by few researchers (e.g., El-Jack, 2003; Hataf et al., 2018; Khatami and O'Kelly, 2013; Patil et al., 2011). To the best of our knowledge, there are few reports on the usages of AG and CH as SAs. For example, Mohamed (1999) reported that AG significantly increased the WAS compared with the reference soil. El-Jack (2003) also showed that AG increased the water retention (insignificantly) and WAS (significantly) and decreased the saturated hydraulic conductivity (K_s) (insignificantly) of three different soils with low, medium, and high clay contents compared with the reference soil. The increase in soil water retention may be due to the effect of gum on improvement of soil structure, leading to more water absorption, or due to the capacity of AG itself to store water. The increase in WAS might be caused by polysaccharides on cementation of soil particles. On the other hand, Hataf et al. (2018) used CH as soil stabilizer and showed that CH provided extra interparticle interaction under wet conditions soon after amendment and this effect reduced over time. The same

authors showed that aggregates of CH-amended soils were instable at dry condition.

The current work investigated the effect of AG and CH on PSD and the possible soil improvements with respect to water retention. To investigate the PSD of soils amended by CH and AG, NMRR was applied. The results from NMRR are underpinned by conventional soil physical and chemical measurements, including WRC, zeta potential (ζ), and saturated water content (θ_s), as well as soil electrical conductivity (EC), organic carbon (OC) content, and measurements of the soil respiration rate (R_s).

Materials and Methods

Soil Sampling

Soil samples were taken from Dryland Agricultural Research Institute (37°12′ N, 46°20′ E, 1730 m asl), 25 km east of Maragheh, East Azerbaijan Province, Iran. Soil samples were collected from depths of 0 to 25 cm. The reference soils were classified as loam texture (25% <2 μm, 33% 2–50 μm; 42% 50–2000 μm), 0.54% OC, EC of 252 μS cm^{-1}, and pH of 6.72.

The soil (fine, mixed, mesic, Typic Calcixerepts based on the USDA system and Calcisols based on the FAO system) (Hemmat and Eskandari, 2004) consists of 42% sand, 33% silt, and 25% clay. Therefore, the soil texture class can be characterized as loamy according to the USDA soil classification. The soil is poor in OC content with 0.5 mass %, and the EC value of 252 μS m^{-1} indicates a normal, nonsaline soil. According to Iran Meteorological Organization report (http://www.irimo.ir), the long-term average annual temperature and precipitation of the region are 13.2°C and 310 mm, respectively. Based on the thermal and moisture regime maps of Iran's soils, the study area has xeric and mesic regimes (Hemmat and Eskandari, 2004).

Laboratory Measurements

Biopolymer Application

In this experiment, biopolymers were dissolved in tap water at a concentration of 25 and 50 g L^{-1}. For CH, the solution was acidified by adding 1 mL acetic acid to obtain a pH of around 5. These solutions (200 mL kg^{-1}) were sprayed on disturbed soil material (<2 mm) and mixed simultaneously by a glass rod. The blank soil was treated similarly by spraying and mixing it with tap water only (200 mL kg^{-1}). After 3 wk of incubation time, we conducted the laboratory measurements. During incubation, soils were air dried and wetted by capillary rise several times by keeping soil water content near field capacity.

Soil Water Retention Curve

The soil WRC was measured using the HYPROP system (UM) as described by Schindler et al. (2010). Cylinders (250 cm^3) were filled to known bulk density (D_b) of 1.2 ± 0.02 g cm^{-3} with dry soil/amendment mixtures. To do this, we transferred 300 g dry soil in small lots into the cylinder to fill it. For uniform packing, we tapped the cylinder gently with each addition of soil during filling process. Packed soils were incubated for 3 wk and then saturated over the course of 2 wk from below by setting the samples into a water bath. After full saturation, the samples were settled on the HYPROP system, and the tensiometer values were recorded permanently in predefined intervals (from 1 to 10 min). The gravimetric water content, θ_m, of the samples was determined by settling the system on a balance at least five times a day. The mean soil suction (h in cm) was calculated from the tensiometer readings for each water content measurement. Because the application of HYPROP system allowed a partial WRC measurement (0–100 kPa), we used the measured θ_v–h data pairs to fit the van Genuchten (1980) equation and then to extrapolate the unmeasured (h > 100 kPa) part of the WRC:

$$\theta_v = \theta_r + \frac{\theta_s - \theta_r}{\left(1+|\alpha h|^n\right)^m} \quad [1]$$

where θ_v (cm^3 cm^{-3}) is volumetric water content ($\theta_m \times D_b$) at each given h (cm); θ_r and θ_s are the residual and saturated volumetric water contents (cm^3 cm^{-3}), respectively; α is the reciprocal of the air-entry value (cm^{-1}); and n and m (both dimensionless) are shape parameters, with $m = 1 - 1/n$. Fitting was performed with the data solver application in Microsoft Excel.

Nuclear Magnetic Resonance Relaxometry

The T_1 and T_2 relaxation times of water in the soil samples were measured in a custom-made Halbach magnet at a field strength of 0.15 T (Raich and Blümler, 2004) operated by a Kea^2 Spectrometer and Prospa software (Magritek). Applying the same procedure described in previous section, core samples were prepared by packing 16.3 g dry reference and biopolymer-amended soils into glass tubes (inner diameter, 24 mm; height, 30 mm) to reach a bulk density of 1.20 ± 0.02 g cm^{-3}. Similar to other experiments, packed soils were incubated for 3 wk and then subjected to NMR measurements. The T_2 spectra were measured using a Carr–Purcell–Meiboom–Gill (CPMG) pulse sequence with up to 4096 echoes spaced at t_E = 0.12 ms (Carr and Purcell, 1954; Meiboom and Gill, 1958). The repetition time was 2000 ms, and up to 128 echo trains were accumulated to improve the signal-to-noise ratio. To determine T_1, we used a saturation recovery pulse sequence (T_1-SR-Add) with CPMG pulse sequence detection with exponentially increasing encoding times between 0.4 and 1000 ms. The T_1 recovery curve was recorded with 16 logarithmically spaced saturation delays with a maximum delay of 1000 ms. All resulting relaxation curves were analyzed by inverse Laplace transformation embedded in the Prospa software, and the resulting relaxation time spectra are represented by the probability distribution $P(\log T_{1,2})$.

The interpretation of the relaxation spectra proceeded on the empirical model of Brownstein and Tarr (1977), which relates the observed relaxation rates to the pore surface to volume ratio $(S/V)_{pore}$:

$$\frac{1}{T_{1,2}} = \frac{1}{T_{1,2,bulk}} + \rho_{1,2}\left(\frac{S}{V}\right)_{pore} + \left(\frac{1}{T_{2,diff}}\right) \quad [2]$$

where ρ is the surface relaxivity parameter, and the subscript indices 1 and 2 refer to longitudinal or transverse relaxation rates and surface relaxivities, respectively. The third term on the right hand side of Eq. [2] signifies the decay of the signal due to translational diffusion in magnetic field gradients, which is expressed in the short time regime as (Mitchell et al., 2010):

$$\frac{1}{T_{2,\mathrm{diff}}} = \frac{D}{12\left(\gamma G t_{\mathrm{E}}\right)^2} \quad [3]$$

where D denotes the molecular translational diffusion coefficient, G is the magnetic field gradient strength, and t_{E} is the inter-echo spacing. This contribution can be minimized by the choice of a sufficient short value for t_{E}.

Determination of Pore Size Distribution from Relaxation Spectra

According to Eq. [2], the average relaxation times are related to the average pore size parameter (S/V) and to its distribution function. In the case that independent information about the pore diameter distribution is available (e.g., from WRC), the surface relaxivity parameters in Eq. [2] can be fitted by matching PSD functions, recalculated from NMRR relaxation time distributions to those obtained from the WRC curves (Stingaciu et al., 2010). Therefore, we translated the WRC into PSD using discrete retention points.

Additional Soil Physical Measurements

Additional soil physical characteristics were measured to support the effects of biopolymer amendment in soils and to help to understand the findings from the NMRR experiments. The examined soil characteristics are soil texture, soil EC, pH, θ_s, ζ, OC content, and R_s measurements.

Soil texture was determined by hydrometer method (Gee and Or, 2002), soil EC, and pH in paste saturation extracts by EC meter and pH meter, and θ_s was determined by weighing a defined volume of soil after full saturation by capillary rise from bottom and oven dried at 105°C.

The ζ, defined as the potential at the shear plane, was measured using the Zetasizer Nano ZS instrument (Malvern Instruments Ltd) (Zelazny et al., 1996). To do this, 100 g of soil plus 200 g H_2O was put into a 1-L glass bottle and shaken for 6 h upright on a horizontal shaker at 150 rpm. Then, another 600 g H_2O was added, and the bottle was shaken to homogenize the mixture. The suspension was left for 6 min, and all particles >20 μm settled to a depth below 12 cm. The supernatant was removed with a pipette and transferred into a new 1-L glass bottle, and a magnetic stick was added. The bottle was put onto a magnetic stirrer that was controlled by a timer. The suspension was slurred for 2 min. A sedimentation time of 12 h allowed the microaggregate phase (particle diameter, 2–20 μm) to separate. After 12 h, the supernatant (the colloidal phase with particle diameter <2 μm) was removed with a pipette and transferred to a new 0.5-L glass bottle. A diluted colloidal phase was then used for ζ measurement by the Zetasizer. Because the ionic strength and pH value of the soil electrolyte solution affect the ζ potential, a portion of the soil colloidal phase was centrifuged using a refrigerated centrifuge for 90 min at 8000 rpm and 20°C. The soil electrolyte section (i.e., the supernatant) was separated, and the ionic strength and pH value of the solution were determined.

The OC content of soil samples was measured according to Nelson and Sommers (1982) based on the wet combustion approach to determine the amount of CO_2 liberated from organic C through the titrimetric technique.

Soil respiration rate was measured over the course of 31 d in a closed chamber using alkali traps to absorb CO_2 (Bekku et al., 1997). To do this, 100 g of dry weight equivalent soil was put into the microcosms and wetted up to a water content of 0.2 g^{-1} soil. The respiration experiment was performed at constant temperature of 20°C. The data from incubation experiments were fitted to single-pool model to predict the decomposition rate constant (k) (d^{-1}), half-life (HL) (d), and mean residence time (MRT) (d) of the organic C turnover for each amended soil as well as for the reference soil as recommended by Weihermüller et al. (2018):

$$C_t = C_0 \exp\left(-kt\right) \quad [4]$$

$$\mathrm{HL} = \frac{\ln\left(2\right)}{k} \quad [5]$$

$$\mathrm{MRT} = \frac{1}{k} \quad [6]$$

where C_t is the cumulative CO_2 evolved at time t (mg g^{-1}), and C_0 is the total CO_2 flux at t_{end} (mg g^{-1}).

Statistical Analysis

A completely randomized design was performed with five treatments and three replications. Treatments included soil amendment by 10 (high, indicated by H) and 5 (low, indicated by L) grams of CH and AG per kg soil (CH-H, CH-L, AG-H, and AG-L) as well as pure soil as reference (hereafter referred to as "reference soil"). The measured variables were subjected to ANOVA to evaluate the differences in measured soil parameters caused by soil amendments, and the Duncan (1955) method was used to conduct comparisons of means.

Regarding the relaxation times spectrums, both peak values (being related to mean value of the pore size) and their probability values (being related to their abundance) are important to interpret the effects of biopolymer amendment on examined soil. Therefore, both peak values and the integral relative area under curve (AUC) were determined. The latter parameter is defined as $\mathrm{AUC}(i) = A_i/A_t$, where A_i is area below the curve between two consecutive minimum values for each peak value, and A_t is area below the entire curve. More specifically, in the case of the T_2 spectrum with three peaks, AUC(1), AUC(2), and AUC(3) are proportional to the water content in interlayer pores, capillary pores, and macropores, respectively. In the other words, AUC(1), AUC(2), and AUC(3)

are proportional to the fractional saturation of the examined soils, being equivalent to the total amount of water in the corresponding pores. The summation of AUC(1), AUC(2), and AUC(3) corresponds to the total porosity derived from NMRR measurements (n_{NMRR}). The peak values (i.e., the relaxation times) and their corresponding AUC values for each treatment were determined and subjected to ANOVA and comparisons of means.

Results and Discussion

Nuclear Magnetic Resonance Relaxometry Results

The averaged probability distribution functions of relaxation spectrum for reference soil and soils amended by biopolymers are plotted in Fig. 1. Probability distribution functions are bimodal for T_1, having two peak values representing $T_1(1)$ and $T_1(2)$, and trimodal for T_2, having three peak values representing $T_2(1)$, $T_2(2)$, and $T_2(3)$ that correspond to different classes of pores (Fig. 1).

Water associated with clay particles or residing in the interlayer space results in T_2 in the range of few milliseconds for very different soil materials, whereas the association of modes with longer relaxation times is not straightforward and depends strongly on the type and texture of soil as well as on swelling and shrinking processes. Subject to a later clarification, we will base our work on the definition of Morriss et al. (1997) and identify $T_2(1)$ with clay-associated water. This is approximately identical to the definition of Meyer et al. (2018) of water relaxing faster than 4.5 ms as micro- and medium-pore water. Water fractions relaxing slower are referred to in this scheme as capillary-pore and macropore water or, in the definition of Meyer et al. (2018), as macropore water. The differentiation between capillary pore and macropore water is arbitrary because the boundaries are not clearly defined. This range corresponds to the range of pore sizes that are easily measurable by WRC. Therefore, it is used for the derivation of surface relaxivities by rescaling NMR-derived PSD to WRC-derived PSD.

Based on the above discussion, $T_1(1)$ and $T_2(1)$ in our experiments at 3 and 1 μs, respectively, correspond to clay-associated water molecules or the presence of interlayer pores, whereas $T_2(2)$ and $T_2(3)$ reflect the effects of the capillary pore–associated and macropore-associated water molecules on transversal relaxation times, respectively; $T_1(2)$ also reflects the simultaneous effects of capillary pores and macropores associated water molecules on the longitudinal relaxation time (Shi et al., 2017).

The variation in the T_1 spectrum under amended soils compared with the reference soil is small and insignificant due to the low resolution of the basic datasets using 16 inversion times (Fig. 1). Therefore, because T_2 spectra had higher resolution, we focused on the variations in T_2 spectrum because T_2 gives more detailed information about the changes in pores related to capillary pores and macropores by differentiating their relaxation times.

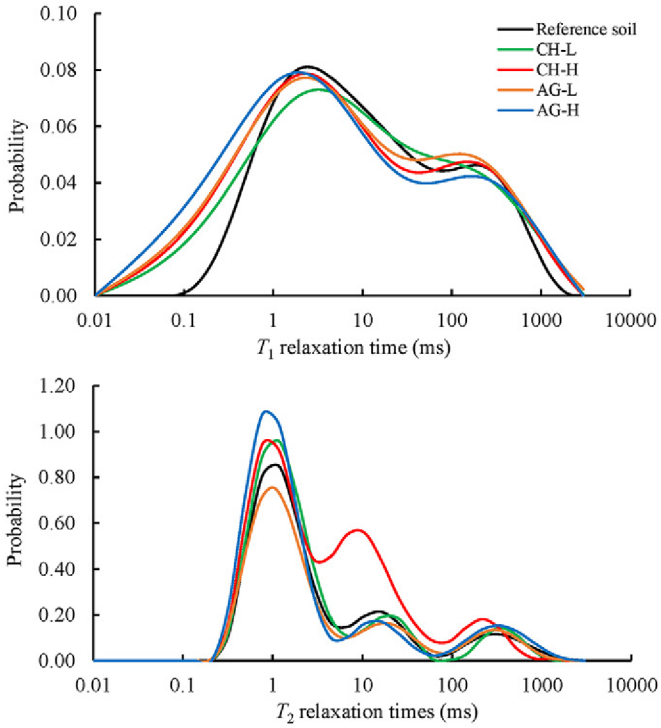

Fig. 1. Longitudinal relaxation time (T_1) and transversal relaxation time (T_2) distribution functions for soils amended with 10 (high, indicated by H) and 5 (low, indicated by L) g of chitosan (CH) and Arabic gum (AG) kg^{-1} soil.

Peak values and their corresponding relative abundances, which are reflected in the AUC values of T_2, were determined and subjected to ANOVA. The results in Table 1 show that the application of AG-H and CH-H slightly but significantly shifted $T_2(1)$ to smaller values (0.8 and 0.9 ms, respectively) compared with the reference soil [$T_2(1)$ = 1.2 ms] (Fig. 2), indicating a reduction of average pore size because the relaxation rate is linearly related to the inverse pore size according to the Brownstein–Tarr model. The two other treatments (CH-L and AG-L) had no effect on $T_2(1)$, showing a $T_2(1)$ around 1.2 ms (Fig. 2). There is no clear reason why the AG-H and CH-H amendment resulted in faster relaxation times in clay-associated water molecules (interlayer pores).

Table 1. Analysis of variance of longitudinal relaxation time (T_2) and relative area under curve (AUC) values among different amendments.

		Mean squares					
Variation	df	AUC (1)†	AUC (2)	AUC (3)	T_2 (1)	T_2 (2)	T_2 (3)
Amendment	4	0.002*	0.029**	0.0001 ns	0.091**	24.91 ns	11278.6**
Error	10	0.0003	0.003	0.0001	0.011	22.68	1250.88

* Significant at the 0.05 probability level; ns, not significant.
** Significant at the 0.01 probability level.
† Numbers in parentheses donate three peak values in the T_2 relaxation time spectrum.

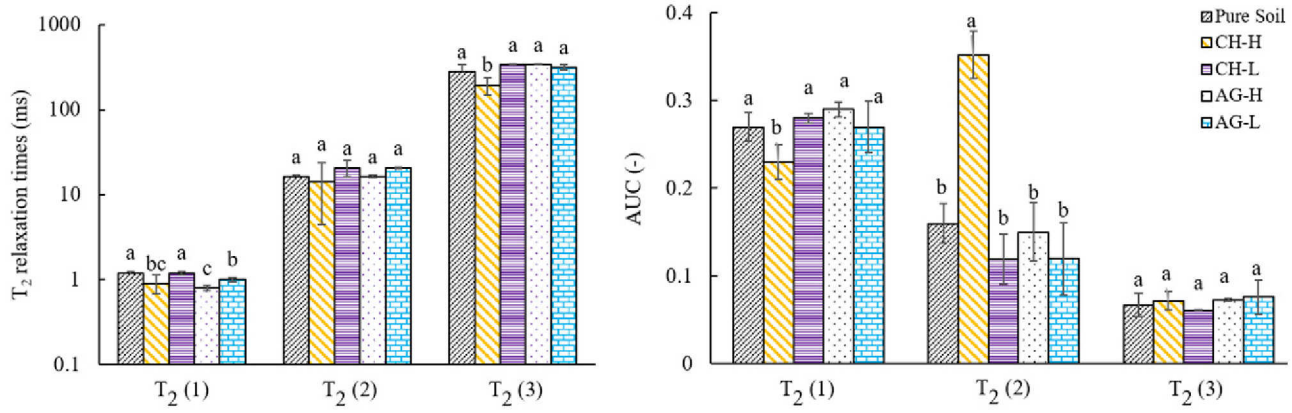

Fig. 2. Comparison of the mean transversal relaxation time (T_2) values and their corresponding relative area under curve (AUC) values for the reference soil and soil amended by biopolymers. CH, chitosan; AG, Arabic gum. For soil amendments, L refers to low (5 g kg^{-1} soil) and H refers to high (10 g kg^{-1} soil).

The results also revealed that CH-H insignificantly resulted in faster relaxation in $T_2(2)$, showing a value of 14 ms compared with 16 ms under reference soil and AG-H. Both lower doses of applied biopolymers (AG-L and CH-L) resulted in insignificantly slower relaxation times for capillary-bound water molecules, showing a $T_2(2)$ value of 21 ms for both compared with 16 ms for the reference soil. The CH-H treatment also resulted in a significantly faster relaxation time in macropore-related water molecules, showing a $T_2(3)$ value of 194 ms compared with 281 ms for the reference soil. The AG-L, AG-H, and CH-L amendments insignificantly increased the relaxation times of $T_2(3)$, showing $T_2(3)$ values of 317 to 341 ms compared with the reference soil with [$T_2(3)$, 281 ms]. Faster relaxation means that the CH-H has narrowed the pores diameters in both micropores (insignificantly) and macropores (significantly) and that AG-H insignificantly narrowed pore diameter in micropores and widened pore diameter in the macropore range.

The effect of CH-H on the pores system becomes more obvious by taking into account the AUC values. The comparison of mean values (Table 1) revealed that CH-H significantly increased the AUC value under $T_2(2)$ (AUC = 0.35), illustrating an increase in the abundance of water bound by capillary forces compared with the reference soil and AG-L, AG-H, and CH-L, with AUC values of 0.14 ± 0.02. The total porosity derived from the T_2 measurement (n_{NMRR}) is reported in Fig. 3, which shows that CH-H had the highest n_{NMRR} value of 0.65 (dimensionless), compared with AG-H and pure soil [n_{NMRR}, 0.52 (dimensionless)] and with AG-L and CH-L [n_{NMRR}, 0.49 (dimensionless)]. Figure 3 also shows the correlation between the n_{NMRR} and θ_s, with an R^2 value of 0.798. Excluding CH-H with an n_{NMRR} value of 0.65 and a θ_s value of 0.54, the n_{NMRR} and θ_s values for other treatments nearly match perfectly. The greater differences between the n_{NMRR} and θ_s values of CH-H treatment are unclear and need to be investigated more in depth. Taking into account the results of the WAS and mean weight diameter (MWD) of the aggregate as published by Rahmati and Kousehlou (2019) for the same soil and treatments, CH-H resulted in more stable but smaller aggregates. One could expect higher abundance of the intermediate or capillary pores, which is in line with NMRR results. The slightly higher saturated water content, θ_s, under CH-H treatment confirms this interpretation and is discussed in more detail below.

Biopolymer Effects on Soil Physicochemical Properties

The biopolymer-related changes in physicochemical properties of the amended soils were investigated to help interpret the NMRR results. The changes in physicochemical properties were analyzed using ANOVA (Table 2). Significant differences were detectable in nearly all measured soil properties except soil pH. We expected lower pH in CH-H– and CH-L–amended soils because the raw biopolymer CH was acidified using acetic acid to solve chitosan in solution. However, this impact is negligible when the CH is added to the soil due to the buffering capacity of the soil.

Comparison of the mean values (Table 3) revealed that θ_s content under CH-H (0.54 cm^3 cm^{-3}) was slightly higher than that under AG-H (0.52 cm^3 cm^{-3}) and the reference soil

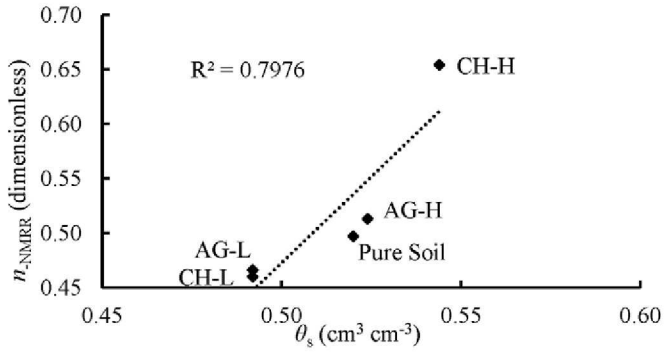

Fig. 3. Correlation between total porosity derived from nuclear magnetic resonance relaxometry measurement (n_{NMRR}) and measured saturated water content (θ_s). CH, chitosan; AG, Arabic gum. For soil amendments, L refers to low (5 g kg^{-1} soil) and H refers to high (10 g kg^{-1} soil).

Table 2. Analysis of variance results for the physicochemical and biological properties of reference soil and soils amended by chitosan and Arabic gum.

Variation	Parameters†						
	df	θ_s	OC	ζ	pH	$EC_{colloid}$	$EC_{electrolyte}$
Amendment	4	0.001*	0.197**	4.358**	0.009 ns	10,194*	11,476*
Error	10	0.0003	0.004	0.475	0.023	2833	3263

* Significant at the 0.05 probability level; ns, not significant.
** Significant at the 0.01 probability level.
† df, degrees of freedom; $EC_{colloid}$, electrical conductivity of colloid section of soil; $EC_{electrolyte}$, electrical conductivity of electrolyte section of soil; OC, organic carbon; θ_s, saturated water content; ζ, zeta potential.

Table 3. Analysis of variance results for respiration data of the reference soil and soils amended by chitosan (CH) and Arabic gum (AG).

Variation	Parameters†				
	df	k_1	C_1	HL	MRT
Amendment	4	0.0004**	47.84**	2874.07**	5988**
Error	10	0.0000	0.0048	15.67	35.8

** Significant at the 0.01 probability level.
† C_1, organic carbon content at time zero; df, degrees of freedom; $k1$, degradation rate constant; HL, half-life; MRT, mean residence time.

(0.52 cm^3 cm^{-3}), indicating that the total porosity did not change significantly by adding the AG-H but slightly increased (insignificantly) under CH-H. On the other hand, treatment with AG-L and CH-L significantly decreased θ_s content, and therefore total porosity, with 0.49 cm^3 cm^{-3} for both treatments. Packing density (bulk density), particle size distribution, particles shapes, and cementing agent are important factors affecting soil porosity (Nimmo, 2004). The observation that bulk density, particle size distribution, and particles shape are not influenced by soil amendment indicates that the total porosity changes are induced by changes in pores and aggregates shapes due to cementation after biopolymer addition. Cementation of soil particles into aggregates and generation of intra-aggregate pore spaces has been observed for organic and clay rich soils. Accordingly, relatively higher total porosities for AG-H and CH-H amendments were expected because they both have organic origins. It seems that CH-H resulted in higher total porosity than AG-H because it has narrowed pores (diameters) in the capillary range as well as macropores, whereas the AG-H amendment has narrowed the pores in the capillary range but widened the macropores, resulting in a lower increase in soil porosity compared with the CH-H treatment. On the other hand, both AG-L and CH-L showed slower relaxation times in the capillary-bound range, meaning that they have widened pores in the capillary bound range. This process is probably responsible for the decrease in total porosity for these amendments. Our partial water retention curve measurements (0–100 kPa) performed for the reference and CH-H– and AG-H–amended soils (Fig. 4) confirm the changes in the pores of the capillary-bound range and macropores to some extent. The retention curve measured for the AG-H–amended soil is close to that measured for the reference soil irrespective of differences in total porosity, whereas the CH-H caused considerable changes in the pore spectra, as reflected by the differences over the entire retention curve (Fig. 4). The impacts of the amendments are discussed in depth below.

To analyze if the biopolymer amendment affected the range of PSD, we discuss previously published results of WAS and MWD of aggregates for the same soil and treatments by Rahmati and Kousehlou (2019). They showed that both CH-H and AG-H treatments increased aggregate stability compared with the reference soil, showing WAS values of 71 and 78%, respectively, vs. 23% for the reference soil, whereas an opposite effect was observed for the MWD (Fig. 5), showing smaller aggregate size under CH-H amendment (MWD = 0.4 mm) and larger aggregate size under AG-H amendment (MWD = 4.1 mm). The reference soil showed a mean MWD value of 2.2 mm. The increase in WAS indirectly confirms the changes in interaggregate formation, which took place in both AG-H and CH-H treatments. On the other hand, smaller MWD under CH-H compared with the reference soil and AG-H confirms the higher frequency of narrower pores under CH-H, which is in line with NMRR results.

The reason for the aggregate size increase under AG-H amendment seems to be clear because Sandford and Baird (1983) stated that polysaccharides can act as binding agents in soils. In fact, polysaccharides and polyacrylic amides bind to each other and act as a bridge for bonding clay minerals. Because AG has a gelatinous and adhesive state, it clogs up soil particles and facilitates aggregate formation and thereby improves soil structure (Whistler, 2012; Whistler and Hymowitz, 1979). Gardner (1972) reported that natural polymers, including AG, stabilize the soil structure, thereby improving aggregate formation and leading to better soil aeration, faster water flow, and improved germination of plants. However, reduced aggregate sizes accompanied by increased aggregate stability after CH-H seems to be more complex to describe. The main reason for reduced aggregate size can be explained by the reduction in the absolute value of soil ζ. The absolute value of ζ under CH-H treatment is smaller (18.5 mV) compared with the

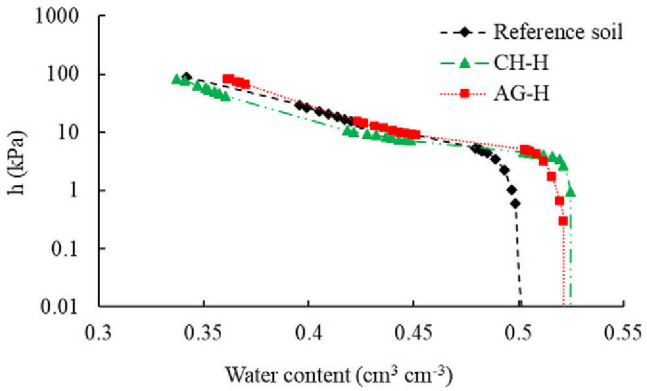

Fig. 4. Measured soil water retention curves for the reference soil the soils amended by 10 g kg^{-1} soil chitosan (CH-H) and Arabic gum (AG-H).

reference soil (20 mV) and the soil amended by AG-H (21.6 mV) (Table 3). It seems that by decreasing ζ, the thickness of the diffuse layer is reduced and the soil becomes more densely packed, especially in the aggregates, as found by Hunter (2013). On the other hand, the aggregates seem to break down into smaller but more stable ones due to the increase of flocculation centers. This hypothesis is confirmed by visual inspection of the soil structure because the soil was puffy under CH but cloddy under AG amendment (Fig. 5).

The ζ can be influenced by pH, exchangeable sodium, and salt concentration (Lebron and Suarez, 1992), but salt concentration also has a significant effect on the ionic strength. The reason for the decrease in absolute value of ζ under CH-H amendment could be related to neutralization of charged particles or ionic strength. Ionic strength of the different amended soils was determined by EC measurements of the colloid fraction. The average ionic strengths of the reference soil and the CH-H, CH-L, AG-H, and AG-L treatments were 0.0015, 0.003, 0.0015, 0.0013, and 0.0014 mol L^{-1}, respectively. However, the ζ potentials of the treated soils were −20.0, −18.5, −20.8, −21.6, and −21.1 mV, respectively. Solubility of CH is probably higher compared with AG in the pore water of the soils. At increased dosage of each amendment, CH is more effective than AG in increasing ionic strength: ionic strength increased significantly from 0.0015 to 0.003 mol L^{-1} in the CH-L– and CH-H–amended soils, respectively, whereas the changes were not noticeable by increasing the dosage of AG from AG-L to AG-H. Nonsignificant changes in ζ in the AG-amended soil with respect to increased dosage can be related to a higher colloidal stability in AG amendments than in CH amendments. Previously published results showed that AG amendment caused more colloidal stability than CH amendment in comparison to a reference soil (Rahmati and Kousehlou, 2019). The value of the ζ can be used as an estimate of the diffuse layer potential and is important in discussing the tendency for the soil colloids to disperse. In other words, by increasing ionic strength, the thickness of the electrical double layer is reduced, and thus soil colloids tend to flocculate. In general, there is a relationship between the effect of salt concentration on ζ and K_s: the higher the ζ, the higher the K_s (Aydin et al., 2004). Decreased K_s can be related to the probable increase in thickness of the diffuse double layer (Aydin et al., 2004). The results indicated that CH-H caused the highest K_s compared with all other amendments (Rahmati and Kousehlou, 2019).

Since CH and AG have organic origins, we evaluated the changes in OC content of the examined soils and mixtures. Both AG-H and AG-L significantly increased OC contents, whereas CH-H and CH-L had no significant effects on OC content. However, this opposed our expectations because we expected a higher OC content under all treatments compared with reference soil. The likely reason that AG and CH amendments increase OC differently could be the different amounts of C atoms in the molecule structures. The different quality and the accessibility of the C atoms for biodegradation in AG- and CH-amended soils could be another reason for slower biodegradation of AG in the soil. To

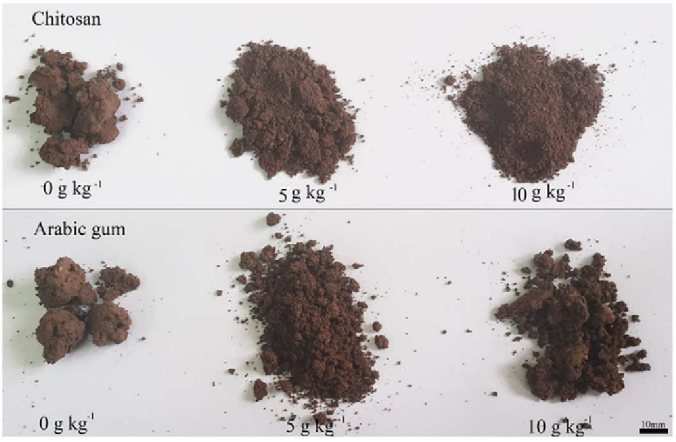

Fig. 5. Aggregate sizes formed by the application of different amounts of chitosan (CH) and Arabic gum (AG). The photo is taken by Nikon D80FLR digital camera with an 18- to 135-mm lens and with a magnification ratio of 1:5.

evaluate this hypothesis, we examined the soil R_s as a measure of microbial activity, being sensitive to the quality and the accessibility of the C atoms in organic structures (Weihermüller et al., 2018). The cumulative CO_2 flux rates over time under reference soil and soils amended by CH and AG (Fig. 6) showed that soil amended with CH-H and CH-L considerably increased the R_s compared with the reference soil or with the soils amended by AG. In addition to visual inspection, we fitted the measured CO_2 flux rates to a single-pool model (Eq. [4]) to estimate the k, HL, and MRT for each amendment and the reference soil. The results were subjected to ANOVA to explore the differences among amended soils and the reference soil. The measured incubation data could be accurately fitted to the single-pool model, with R^2 values of 0.84 to 0.99 and RMSE values of 0.15 to 0.89 mg g^{-1}. The ANOVA results (Table 4) show that the kinetic parameters k, HL, MRT, and C_1 significantly differ between reference soil and soil amended by CH and AG. Comparisons of means (Table 5) show that the decomposition rate constant of the reference soil (k = 0.035 d^{-1}) is significantly higher than the amended soils; AG-H showed the

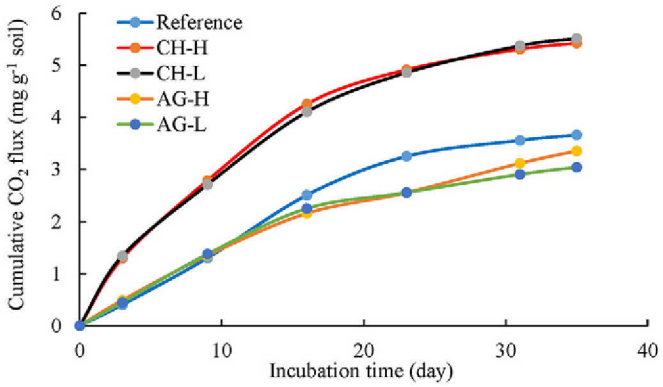

Fig. 6. Cumulative CO_2 flux rates over time for the reference soil and for soil amended with chitosan (CH) and Arabic gum (AG). For amendments, L refers to low (5 g kg^{-1} soil) and H refers to high (10 g kg^{-1} soil).

Table 4. Comparison of means of physicochemical properties of the reference soils and the soils amended by low and high dosages of chitosan (CH-L and CH-H) and Arabic gum (AG-L and AG-H).

Treatment†	Parameters‡				
	ζ	$EC_{colloid}$	$EC_{electrolyte}$	OC	θ_s
	mV	dS m^{-1}		%	cm^3 cm^{-3}
Reference soil	−20.0 (b)§	118 (b)	104 (b)	0.54 (c)	0.520 (ab)
CH-H	−18.5 (a)	241 (a)	232 (a)	0.63 (c)	0.544 (a)
CH-L	−20.8 (bc)	116 (b)	96 (b)	0.55 (c)	0.492 (b)
AG-H	−21.6 (c)	103 (b)	86 (b)	1.11 (a)	0.524 (ab)
AG-L	−21.1 (bc)	108 (b)	91 (b)	0.95 (b)	0.492 (b)

† For amendments, L refers to low (5 g kg^{-1} soil) and H refers to high (10 g kg^{-1} soil).
‡ $EC_{colloid}$, electrical conductivity of colloid section of soil; $EC_{electrolyte}$, electrical conductivity of electrolyte section of soil; OC, organic carbon; θ_s, saturated water content; ζ, zeta potential.
§ The letters a, b, and c represent different groups with mean values from greater to less. Combined letters indicate that there is no difference between the two related groups.

Table 5. Comparison of means of respiration data the reference soils and the soils amended by low and high dosages of chitosan (CH-L and CH-H) and Arabic gum (AG-L and AG-H).

Treatment†	Parameters‡			
	k_1	C_1	Half-life	MRT
	d^{-1}	mg g^{-1}	d	
Reference soil	0.035 (a)§	5.36 (e)	20 (d)	29 (d)
CH-H	0.012 (c)	14.48 (b)	57 (b)	82 (b)
CH-L	0.022 (b)	9.60 (d)	33 (c)	47 (c)
AG-H	0.007 (d)	15.13 (a)	101 (a)	145 (a)
AG-L	0.012 (c)	10.07 (c)	60 (b)	86 (b)

† For amendments, L refers to low (5 g kg^{-1} soil) and H refers to high (10 g kg^{-1} soil).
‡ C_1, organic carbon content at time zero; HL, half-life; k_1, degradation rate constant; MRT, mean residence time.
§ The letters a, b, c, and d represent different groups with mean values from greater to less.

lowest decomposition rate (k = 0.007 d^{-1}). As a consequence, the HL and MRT (20 and 29 d) of the reference soil was significantly lower than the amended soils. Treatment with AG-H showed an HL of 101 d and an MRT of 145 d, indicating the most stabilized conditions for the carbon among all treatments. Although CH-H increased the HL (57 d) and MRT (82 d) compared with reference soil, it had insignificantly different values of HL and MRT compared with AG-L with HL and MRT values of 60 and 87 d, respectively. Based on these results, we conclude that CH provides a more easily degradable carbon source to the soil microbial community compared with AG or the native carbon stock available in the reference soil. Therefore, parts of the applied CH can be easily decomposed during the 4-wk experiment. Although CH amended into the soil was partially decomposed, it still affected the other soil properties studied. However, the interaction between microbial degradation and changes in soil properties are not fully understood. On the other hand, AG showed less CO_2 flux during incubation but showed the smallest effect on the other soil properties studied compared with CH, indicating that the microbial turnover and the impact of soil property changes are interlinked; these processes are not fully understood. We conclude that AG seems to need much more time to affect soil properties.

Application of AG caused R_s rates lower than those of the reference soil after 2 wk (Fig. 6). This could be caused by the existence of antibacterial compounds in AG or by its higher gelling characteristic (i.e., AG sticks more strongly to soil particles and stays out of the reach of the soil microbial community). The last case could be confirmed by large soil clods (aggregates) created under AG amendment, but this effect needs to be investigated in more depth. The exact mechanisms affecting microbial degradation with AG and CH are not well understood, and more studies are needed to explore whether any toxic effects are detectable or if the amendments cause shifts in the soil microbial community.

Pore Size Distribution from Nuclear Magnetic Resonance Relaxometry Experiments

The PSD functions of the soils were examined by rescaling T_1 and T_2 distribution functions using Eq. [2]. For this purpose, we matched the NMRR-PSD to the WRC-PSD measured with HYPROP in the range of 0 and 100 kPa by adjusting the surface relaxivity parameter. Because the soil amended with AG-L and CH-L showed a negligible effect on NMRR results compared with the reference, we only discuss the results obtained for CH-H and AG-H amendments. Additionally, the measured water retention data were translated to the approximate PSD curves using discrete retention points. Figure 7 illustrates the PSD curves derived from WRC and from T_1 and T_2 distributions for the reference soil and the soil amended by CH-H and AG-H. We did not use the fast relaxation modes for the calculation because these modes were associated with clay-bound water only (organic bound and bound to the biopolymer structures is also possible), and therefore do not provide information of the PSD for water molecules associated with capillary pores and macropores. The effect of the fraction on mineral (clay)-bound water is also not reflected in the WRCs because the measurements only span h < 100 kPa. The fitted van Genuchten parameters, bulk water relaxation times, and surface relaxivity parameters are listed in Table 6. Finally, the weighted mean pore diameter of the reference and amended soils calculated from knowledge of the measured discrete points along the WRC and those obtained by NMRR (T_1 and T_2) are listed in Table 4.

There is satisfactory agreement between predicted rescaled pore diameters from WRC and NMRR measurements showing R^2 values of 0.79 to 0.92 and RMSE of 0.61 to 1.45 μm for T_1 and R^2 values of 0.78 to 0.99 and RMSE values of 0.57 to 1.38 μm for T_2 (Fig. 7). However, for CH-H, the CPMG-derived PSD curve is slightly shifted *vs.* the WRC-derived curve. The T_1 distribution apparently provides less information about the PSD than T_2. On the other hand, T_2 measurements show more detailed

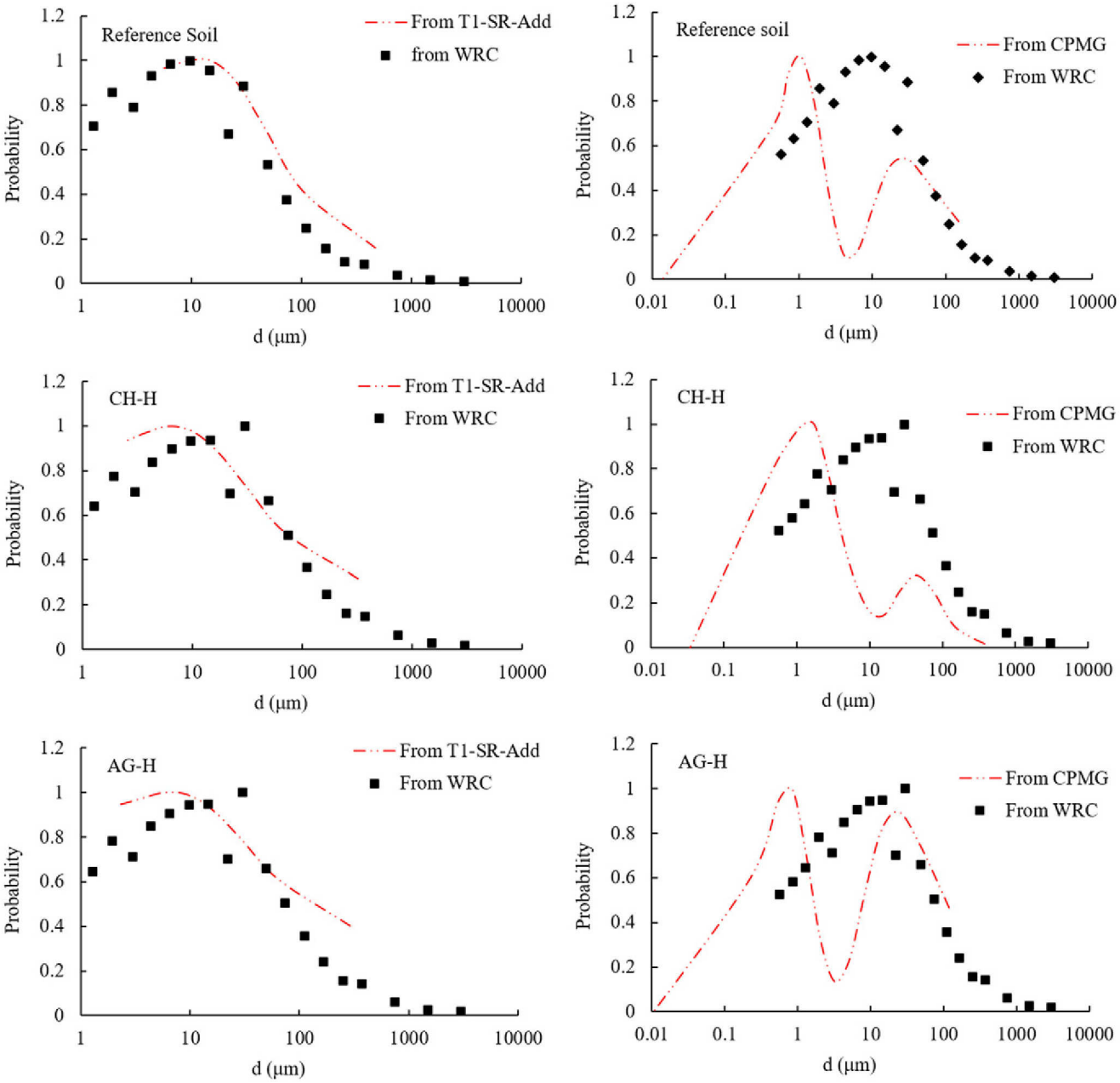

Fig. 7. Comparison between pore size (equivalent cylindrical diameter) distributions from nuclear magnetic resonance relaxometry–derived longitudinal relaxation time (T_1) and transversal relaxation time (T_2) to those determined from measured water retention curves using discrete retention points for the reference and amendments soils. AG-H, Arabic gum at 10 g kg^{-1} soil. CPGM, Carr–Purcell–Meiboom–Gill; T_1-SR-Add, longitudinal relaxation times saturation recovery pulse sequence; WRC, water retention curve.

information about the PSD compared with those obtained from the WRC because T_2 shows a bimodal distribution, which is not shown in the WRC. Therefore, NMRR T_2 measurements contain more information about capillary pores and macropores compared with classical soil water retention curves.

Comparing the PSD for the AG-H– and CH-H–amended soils with the reference soil (Fig. 7) shows that CH-H had more effect on pores where the water was bound by capillary forces, whereas AG-H had more effect on macropores. Although the reference soil and the soils amended by CH-H and AG-H show a mean pores diameter value of 1 μm (the peak values in NMR-derived PSD curve), which is the pore region where the water is hold by capillarity, it seems that CH-H had increased the pore spectrum in this capillary bound region compared with the reference soils, showing wider probability for pore related to capillary-bound water molecules. The weighed mean macropore diameter value was estimated to be 31, 44, and 24 μm for the reference and CH-H– and AG-H–amended soils, respectively. By taking into account the peak values, it seems that CH-H resulted in larger macropores and AG-H in narrower macropores. However, the increased pore sizes under CH-H seems to be compensated by a decrease in the number or the availability of the pores. On the other hand, the

Table 6. The van Genuchten (1980) model parameters obtained from water retention curve measurements and bulk water and pore surface relaxivity parameters from nuclear magnetic resonance relaxometry measurements.

Treatment†	Parameters‡											
	θ_r	θ_s	α	n	m	$T_{1,bulk}$	$T_{2,bulk}$	ρ_1	ρ_2	WRC	T_1	T_2
	—— $cm^3\ cm^{-3}$ ——		cm^{-1}			—— ms ——		—— $\mu m\ s^{-1}$ ——		μm		
Reference soil	0.17	0.50	0.113	1.30	0.23	1500	1300	14	16	34	40	16
CH-H	0.14	0.52	0.178	1.26	0.21	1500	1300	10	41	52	32	13
AG-H	0.21	0.52	0.171	1.27	0.20	1500	1300	9	13	50	33	18

† AG-H, Arabic gum applied at 10 $g\ kg^{-1}$ soil; CH-H, chitosan applied at 10 $g\ kg^{-1}$ soil.
‡ θ_r and θ_s are the saturated and residual volumetric water contents; α is the reciprocal of the air entry value; and n and m are shape parameters, with $m = 1 - 1/n$.

decreased pore sizes under AG-H could also be compensated for by the increase in the number of the availability of the pores.

In general, CH-H decreased the weighted mean value of entire pore sizes compared with the reference soil (d = 13 μm vs. 16 μm), and AG-H increased the weighted mean value of entire pore sizes (d = 18 μm) (Table 4).

Taking into account the water contents at field capacity (FC, in h = 10 kPa from measured data) and permanent wilting point (PWP, from extrapolated data) shows that AG-H decreased the available water (AW = FC − PWP) for plant use, showing FC and PWP values of 0.40 and 0.27 $cm^3\ cm^{-3}$, respectively, compared with those of 0.39 and 0.24 $cm^3\ cm^{-3}$ for the reference soil, whereas CH-H increased the available water calculated from FC and PWP of 0.38 and 0.23 $cm^3\ cm^{-3}$.

Conclusion and Outlook

In this study, we evaluated the effects of two different biopolymers (CH and AG) on the physical and biological properties of a dryland loamy soil. Results from NMRR experiments revealed that AG caused faster NMRR relaxation times in amended soils, indicating an increase of pores with larger diameters compared with the reference soils, whereas CH mostly increased the number and size of pores representing capillary-bound water. These results were confirmed in previous studies where application of both AG and CH significantly increased aggregate stability. However, the size of stable aggregates decreased in CH-amended soils and increased in AG-amended soils compared with reference soils. Application of AG and CH also significantly affected the soil water content, where the water content at FC and PWP from measured data showed that AG-H decreased the AW by changing the FC and PWP to 0.40 and 0.27 $cm^3\ cm^{-3}$, respectively, compared with those of the reference soil with 0.39 and 0.24 $cm^3\ cm^{-3}$. On the other hand, CH-H increased the AW due to changes in FC and PWP to 0.38 and 0.23 $cm^3\ cm^{-3}$, respectively.

The NMRR results revealed that the PSD can be predicted from both T_1 and T_2 measurements in a satisfactory manner, showing reasonably high agreement between PSD obtained from WRC and NMRR measurements, with R^2 values of 0.79 to 0.92 and RMSE of 0.61 to 1.45 μm for T_1 and R^2 values of 0.78 to 0.99 and RMSE values of 0.57 to 1.38 μm for T_2. In general, the T_2 distribution provided more information about the PSD and the WRC compared with T_1 because T_2 showed a bimodal distribution for capillary pores and macropores associated with water molecules, which is not seen in the T_1 and/or WRC distribution.

The results from incubation experiments showed that CH-amended soils had considerably increased respiration rates compared with the reference soil or AG-amended the soils. In addition to respiration rate, we analyzed the effect of biopolymers on soil biological conditions by determining the decomposition rate constant (k), HL, and MRT of all examined soils. In our study, AG-H with an HL of 101 d and MRT of 145 d proved to be more biologically stable in soil compared with the reference soil and the CH-amended soil. Based on these results, CH was more likely to provide more degradable carbon to the soil microbial community than AG.

Our results show that AG and CH significantly affected the hydraulic and structural properties as well as the moisture conditions of the examined soils. Therefore, it seems that these biopolymers can be used to modify the structural properties of loamy soils.

Acknowledgments

This work was supported by the Center for International Scientific Studies & Collaboration (CISSC). Mehdi Rahmati thanks the cooperation from International & Scientific Cooperation Office of University of Maragheh. The support received from the Forschungszentrum Jülich GmbH is gratefully acknowledged by Mehdi Rahmati.

References

Awad, Y., E. Blagodatskaya, Y. Ok, and Y. Kuzyakov. 2013. Effects of polyacrylamide, biopolymer and biochar on the decomposition of 14C-labelled maize residues and on their stabilization in soil aggregates. Eur. J. Soil Sci. 64:488–499. doi:10.1111/ejss.12034

Aydin, M., T. Yano, and S. Kilic. 2004. Dependence of zeta potential and soil hydraulic conductivity on adsorbed cation and aqueous phase properties. Soil Sci. Soc. Am. J. 68:450–459. doi:10.2136/sssaj2004.4500

Barrie, P.J. 2000. Characterization of porous media using NMR methods. Annu. Rep. NMR Spectrosc. 41:265–316. doi:10.1016/S0066-4103(00)41011-2

Bayer, A., H.-J. Vogel, O. Ippisch, and K. Roth. 2005. Do effective properties for unsaturated weakly layered porous media exist? An experimental study. Hydrol. Earth Syst. Sci. 9:517–522. doi:10.5194/hess-9-517-2005

Bekku, Y., H. Koizumi, T. Oikawa, and H. Iwaki. 1997. Examination of four methods for measuring soil respiration. Appl. Soil Ecol. 5:247–254. doi:10.1016/S0929-1393(96)00131-X

Bird, N., A. Preston, E. Randall, W. Whalley, and A. Whitmore. 2005. Measurement of the size distribution of water-filled pores at different matric potentials by stray field nuclear magnetic resonance. Eur. J. Soil Sci. 56:135–143. doi:10.1111/j.1351-0754.2004.00658.x

Bittelli, M., and M. Flury. 2009. Errors in water retention curves determined with pressure plates. Soil Sci. Soc. Am. J. 73:1453–1460. doi:10.2136/sssaj2008.0082

Blanco-Canqui, H. and R. Lal. 2008. Principles of soil conservation and management. Springer, Berlin.

Brax, M., C. Buchmann, and G.E. Schaumann. 2017. Biohydrogel induced soil–water interactions: How to untangle the gel effect? A review. J. Plant Nutr. Soil Sci. 180(2). doi:10.1002/jpln.201600453

Brownstein, K.R., and C.E. Tarr. 1977. Spin-lattice relaxation in a system governed by diffusion. J. Magn. Reson. (1969–1992) 26:17–24.

Brownstein, K.R., and C.E. Tarr. 1979. Importance of classical diffusion in NMR studies of water in biological cells. Phys. Rev. A 19:2446–2453. doi:10.1103/PhysRevA.19.2446

Buchmann, C., M. Meyer, and G.E. Schaumann. 2015. Characterization of wet aggregate stability of soils by H-NMR relaxometry. Magn. Reson. Chem. 53:694–703. doi:10.1002/mrc.4147

Busch, S., L. Weihermüller, J.A. Huisman, C.M. Steelman, A.L. Endres, H. Vereecken, and J. van der Kruk. 2013. Coupled hydrogeophysical inversion of time-lapse surface GPR data to estimate hydraulic properties of a layered subsurface. Water Resour. Res. 49:8480–8494. doi:10.1002/2013WR013992

Carr, H.Y., and E.M. Purcell. 1954. Effects of diffusion on free precession in nuclear magnetic resonance experiments. Phys. Rev. 94:630–638. doi:10.1103/PhysRev.94.630

Chang, I., and G.-C. Cho. 2012. Strengthening of Korean residual soil with b-1, 3/1, 6-glucan biopolymer. Constr. Build. Mater. 30:30–35. doi:10.1016/j.conbuildmat.2011.11.030

Chang, I., J. Im, A.K. Prasidhi, and G.-C. Cho. 2015a. Effects of Xanthan gum biopolymer on soil strengthening. Constr. Build. Mater. 74:65–72. doi:10.1016/j.conbuildmat.2014.10.026

Chang, I., A.K. Prasidhi, J. Im, H.-D. Shin, and G.-C. Cho. 2015b. Soil treatment using microbial biopolymers for anti-desertification purposes. Geoderma 253:39–47. doi:10.1016/j.geoderma.2015.04.006

Duncan, D.B. 1955. Multiple range and multiple *F* tests. Biometrics 11:1–42. doi:10.2307/3001478

El-Jack, E.-M.M.S. 2003. Effect of gum Arabic on some soil physical properties and growth of sorghum grown on three soil types. Univ. of Khartoum, Shambat, Sudan.

Gardner, W. 1972. Use of synthetic soil conditioners in the 1950's and some implications to their further development. Ghent Rijksfac Landbouwetensch Meded 1:1046–1061.

Gee, G.W. and D. Or. 2002. Particle-size analysis. In: J.H. Dane and G.C. Topp, editors, Methods of soil analysis. Part 4. SSSA Book Ser. 5. SSSA, Madison, WI. p. 255–293. doi:10.2136/sssabookser5.4.c12

Hall, L.D., M.G. Amin, E. Dougherty, M. Sanda, J. Votrubova, K.S. Richards, et al. 1997. MR properties of water in saturated soils and resulting loss of MRI signal in water content detection at 2 tesla. Geoderma 80:431–448. doi:10.1016/S0016-7061(97)00065-7

Hataf, N., P. Ghadir, and N. Ranjbar. 2018. Investigation of soil stabilization using chitosan biopolymer. J. Clean. Prod. 170:1493–1500. doi:10.1016/j.jclepro.2017.09.256

Hemmat, A., and I. Eskandari. 2004. Tillage system effects upon productivity of a dryland winter wheat–chickpea rotation in the northwest region of Iran. Soil Tillage Res. 78:69–81. doi:10.1016/j.still.2004.02.013

Hinedi, Z., A. Chang, M. Anderson, and D. Borchardt. 1997. Quantification of microporosity by nuclear magnetic resonance relaxation of water imbibed in porous media. Water Resour. Res. 33:2697–2704. doi:10.1029/97WR02408

Hinedi, Z., Z. Kabala, T. Skaggs, D. Borchardt, R. Lee, and A. Chang. 1993. Probing soil and aquifer material porosity with nuclear magnetic resonance. Water Resour. Res. 29:3861–3866. doi:10.1029/93WR02302

Hollenbeck, K.-J., and K.H. Jensen. 1998. Experimental evidence of randomness and nonuniqueness in unsaturated outflow experiments designed for hydraulic parameter estimation. Water Resour. Res. 34:595–602. doi:10.1029/97WR03609

Hunter, R.J. 2013. Zeta potential in colloid science: Principles and applications. Vol. 2. Academic Press, Cambridge, MA.

Jadoon, K.Z., L. Weihermüller, B. Scharnagl, M.B. Kowalsky, M. Bechtold, S.S. Hubbard, et al. 2012. Estimation of soil hydraulic parameters in the field by integrated hydrogeophysical inversion of time-lapse ground-penetrating radar data. Vadose Zone J. 11(4). doi:10.2136/vzj2011.0177

Jaeger, F., S. Bowe, H. Van As, and G. Schaumann. 2009. Evaluation of 1H NMR relaxometry for the assessment of pore-size distribution in soil samples. Eur. J. Soil Sci. 60:1052–1064. doi:10.1111/j.1365-2389.2009.01192.x

Jonard, F., L. Weihermüller, M. Schwank, K.Z. Jadoon, H. Vereecken, and S. Lambot. 2015. Estimation of hydraulic properties of a sandy soil using ground-based active and passive microwave remote sensing. IEEE Trans. Geosci. Remote Sens. 53:3095–3109. doi:10.1109/TGRS.2014.2368831

Jullien, M., J. Raynal, E. Kohler, and O. Bildstein. 2005. Physicochemical reactivity in clay-rich materials: Tools for safety assessment. Oil Gas Sci. Technol. 60:107–120. doi:10.2516/ogst:2005007

Khatami, H.R., and B.C. O'Kelly. 2013. Improving mechanical properties of sand using biopolymers. J. Geotech. Geoenviron. Eng. 139:1402–1406. doi:10.1061/(ASCE)GT.1943-5606.0000861

Kleinberg, R., W. Kenyon, and P. Mitra. 1994. Mechanism of NMR relaxation of fluids in rock. J. Magn. Reson. A 108:206–214. doi:10.1006/jmra.1994.1112

Koestel, J. 2018. SoilJ: An ImageJ plugin for the semiautomatic processing of three-dimensional x-ray images of soils. Vadose Zone J. 17:170062. doi:10.2136/vzj2017.03.0062

Kowalczyk, P., A.P. Terzyk, P.A. Gauden, R. Leboda, E. Szmechtig-Gauden, G. Rychlicki, et al. 2003. Estimation of the pore-size distribution function from the nitrogen adsorption isotherm. Comparison of density functional theory and the method of Do and co-workers. Carbon 41:1113–1125. doi:10.1016/S0008-6223(03)00019-8

Kutilek, M. 2004. Soil hydraulic properties as related to soil structure. Soil Tillage Res. 79:175–184. doi:10.1016/j.still.2004.07.006

Kutilek, M., and D. Nielsen. 1994. Soil hydrology. Catena Verlag, Cremlingen-Destedt, Germany.

Lebron, I., and D.L. Suarez. 1992. Variations in soil stability within and among soil types. Soil Sci. Soc. Am. J. 56:1412–1421. doi:10.2136/sssaj1992.03615995005600050014x

Lipiec, J., and W. Stepniewski. 1995. Effects of soil compaction and tillage systems on uptake and losses of nutrients. Soil Tillage Res. 35:37–52. doi:10.1016/0167-1987(95)00474-7

Maghchiche, A., A. Haouam and B. Immirzi. 2010. Use of polymers and biopolymers for water retaining and soil stabilization in arid and semiarid regions. J. Taibah Univ. Sci. 4:9–16. doi:10.1016/S1658-3655(12)60022-3

Mallants, D., P.-H. Tseng, N. Toride, A. Tinunerman, and J. Feyen. 1997. Evaluation of multimodal hydraulic functions in characterizing a heterogeneous field soil. J. Hydrol. 195:172–199. doi:10.1016/S0022-1694(96)03251-9

Meiboom, S., and D. Gill. 1958. Modified spin-echo method for measuring nuclear relaxation times. Rev. Sci. Instrum. 29:688–691. doi:10.1063/1.1716296

Meyer, M., C. Buchmann, and G. Schaumann. 2018. Determination of quantitative pore-size distribution of soils with ^{1}H NMR relaxometry. Eur. J. Soil Sci. 69:393–406. doi:10.1111/ejss.12548

Mitchell, J., T. Chandrasekera, and L. Gladden. 2010. Obtaining true transverse relaxation time distributions in high-field NMR measurements of saturated porous media: Removing the influence of internal gradients. J. Chem. Phys. 132:244705. doi:10.1063/1.3446805

Mohamed, B. 1999. Effect of natural amendments on aggregate stability and water flow in different soils. M.S. thesis. Faculty of Agriculture, Univ. of Khartoum, Shambat, Sudan.

Morriss, C., D. Rossini, C. Straley, P. Tutunjian, and H. Vinegar. 1997. Core analysis by low-field NMR. Log Anal. 38(2).

Nelson, D., and L.E. Sommers. 1982. Total carbon, organic carbon, and organic matter. In: A.L. Page et al., editors, Methods of soil analysis. Part 2. Chemical and microbiological properties. 2nd ed. Agron. Monogr. 9. ASA and SSSA, Madison, WI. p. 539–579. doi:10.2134/agronmonogr9.2.2ed.c29

Neyshabouri, M.R., M. Rahmati, C. Doussan, and B. Behroozinezhad. 2013. Simplified estimation of unsaturated soil hydraulic conductivity using bulk electrical conductivity and particle size distribution. Soil Res. 51:23–33. doi:10.1071/SR12158

Nimmo, J.R. 2004. Porosity and pore size distribution. In: D. Hillel et al., editors, Encyclopedia of soils in the environment. Vol. 3. Academic Press, San Diego. p. 295–303.

Orts, W.J., A. Roa-Espinosa, R.E. Sojka, G.M. Glenn, S.H. Imam, K. Erlacher, and J.S. Pedersen. 2007. Use of synthetic polymers and biopolymers for soil stabilization in agricultural, construction, and military applications. J. Mater. Civ. Eng. 19:58–66. doi:10.1061/(ASCE)0899-1561(2007)19:1(58)

Pagliai, M., and N. Vignozzi. 2002. The soil pore system as an indicator of soil quality. Adv. GeoEcology 35:69–80.

Patil, S.V., B. Salunke, C. Patil, and R. Salunkhe. 2011. Studies on amendment of different biopolymers in sandy loam and their effect on germination, seedling growth of *Gossypium herbaceum* L. Appl. Biochem. Biotechnol. 163:780–791. doi:10.1007/s12010-010-9082-1

Peth, S., R. Horn, F. Beckmann, T. Donath, J. Fischer, and A. Smucker. 2008. Three-dimensional quantification of intra-aggregate pore-space features using synchrotron-radiation-based microtomography. Soil Sci. Soc. Am. J. 72:897–907. doi:10.2136/sssaj2007.0130

Pohlmeier, A., S. Haber-Pohlmeier, and S. Stapf. 2009. A fast field cycling nuclear magnetic resonance relaxometry study of natural soils. Vadose Zone J. 8:735–742. doi:10.2136/vzj2008.0030

Pohlmeier A., S. Garré, and T. Roose. 2018. Noninvasive imaging of processes in natural porous media: From pore to field scale. Vadose Zone J. 17:180044. doi:10.2136/vzj2018.03.0044

Rahmati, M., and M. Kousehlou. 2019. Effects of chitosan and Arabic gum biopolymers on some physical properties of swelling soils. Water Soil Sci. Univ. Tabriz (in press).

Raich, H., and P. Blümler. 2004. Design and construction of a dipolar Halbach array with a homogeneous field from identical bar magnets. Concepts Magn. Reson. 23B:16–25.

Ryu, S. 2009. Effect of inhomogeneous surface relaxivity, pore geometry and internal field gradient on NMR logging: Exact and perturbative theories and numerical investigations. arXiv:0906.5327.

Sandford, P.A., and J. Baird. 1983. Industrial utilization of polysaccharides. In: The polysaccharides. Vol. 2. Academic Press, New York. p. 411–490. doi:10.1016/B978-0-12-065602-8.50012-1

Schindler, U., W. Durner, G. von Unold, and L. Müller. 2010. Evaporation method for measuring unsaturated hydraulic properties of soils: Extending the measurement range. Soil Sci. Soc. Am. J. 74:1071–1083. doi:10.2136/sssaj2008.0358

Shi, F., C. Zhang, J. Zhang, X. Zhang, and J. Yao. 2017. The changing pore size distribution of swelling and shrinking soil revealed by nuclear magnetic resonance relaxometry. J. Soils Sediments 17:61–69. doi:10.1007/s11368-016-1511-5

Smet, S., E. Plougonven, A. Leonard, A. Degré, and E. Beckers. 2017. X-ray micro-CT: How soil pore space description can be altered by image processing. Vadose Zone J. 17:160049. doi:10.2136/vzj2016.06.0049

Song, Y.-Q. 2010. Recent progress of nuclear magnetic resonance applications in sandstones and carbonate rocks. Vadose Zone J. 9:828–834. doi:10.2136/vzj2009.0171

Stingaciu, L., L. Weihermüller, S. Haber-Pohlmeier, S. Stapf, H. Vereecken, and A. Pohlmeier. 2010. Determination of pore size distribution and hydraulic properties using nuclear magnetic resonance relaxometry: A comparative study of laboratory methods. Water Resour. Res. 46:W11510. doi:10.1029/2009WR008686

Valentine, T.A., P.D. Hallett, K. Binnie, M.W. Young, G.R. Squire, C. Hawes, et al. 2012. Soil strength and macropore volume limit root elongation rates in many UK agricultural soils. Ann. Bot. 110:259–270. doi:10.1093/aob/mcs118

van Genuchten, M.Th. 1980. A closed-form equation for predicting the hydraulic conductivity of unsaturated soils. Soil Sci. Soc. Am. J. 44:892–898. doi:10.2136/sssaj1980.03615995004400050002x

Webb, P.A. 2001. An introduction to the physical characterization of materials by mercury intrusion porosimetry with emphasis on reduction and presentation of experimental data. Micromeritics Instrument Corp., Norcross, GA.

Weihermüller, L., J. Huisman, A. Graf, M. Herbst, and J.-M. Sequaris. 2009. Multistep outflow experiments to determine soil physical and carbon dioxide production parameters. Vadose Zone J. 8:772–782. doi:10.2136/vzj2008.0041

Weihermüller, L., A. Neuser, M. Herbst, and H. Vereecken. 2018. Problems associated to kinetic fitting of incubation data. Soil Biol. Biochem. 120:260–271. doi:10.1016/j.soilbio.2018.01.017

Whistler, R. 2012. Industrial gums: Polysaccharides and their derivatives. Elsevier, Amsterdam.

Whistler, R.L., and T. Hymowitz. 1979. Guar: Agronomy, production, industrial use, and nutrition. Purdue Univ. Press, W. Lafayette, IN.

Zelazny, L.W., L. He, and A. Vanwormhoudt. 1996. Charge analysis of soils and anion exchange. In: D. Sparks, editor, Methods of soil analysis. Part 3. Chemical methods. SSSA Book Ser. 5. SSSA and ASA, Madison, WI. p. 1231–1253. doi:10.2136/sssabookser5.3.c41

Žydelis, R., L. Weihermüller, M. Herbst, A. Klosterhalfen, and S. Lazauskas. 2018. A model study on the effect of water and cold stress on maize development under nemoral climate. Agric. For. Meteorol. 263:169–179. doi:10.1016/j.agrformet.2018.08.011